Acta Cryst. (1984). A**40**, 264–269

Short-Range-Order Structure of Amorphous Hydrous Erbium Oxide

BY W. O. MILLIGAN, D. F. MULLICA, H. O. PERKINS AND C. K. C. LOK

Departments of Chemistry and Physics, Baylor University, Waco, Texas 76798, *USA*

J. J. MCCOY

Department of Mathematics and Physics, Tarleton University, Stephenville, Texas 76402, *USA*

AND H. A. WOLCOTT

Atlantic-Richfield Co., Dallas, Texas 75221, *USA*

(*Received* 21 *July* 1983; *accepted* 22 *November* 1983)

Abstract

The hydrous lanthanide oxides comprise a complicated series of both crystalline and amorphous compounds. The amorphous short-range-order (SRO) phase of hydrous erbium oxide is the subject of this work. A thorough discussion of the instrumental arrangement and electronic counting chain for the X-radiation diffraction data collection is included. The scattering profiles for hydrous erbium oxide are shown and details of the ensuing data correction procedures are given. A radial distribution analysis of the calculated interference function, $Si(S)$, was performed. SRO interatomic distances and the first-shell coordination number are reported. The mean Er–O bond distance is found to be 2·36 Å and the erbium metal is nine coordinated. Comparison of the experimental radial distribution curve to ones calculated from crystalline systems lend credibility to the experimentally determined distances.

Introduction

Research regarding amorphous lanthanide materials initiated with the works of Joye & Garnier (1912) and Damiens (1918). These investigators reported gelatinous precipitates upon the addition of alkali to aqueous salt solutions of the lower members of the lanthanoid series. Dehydration isobars and X-ray diffraction studies were done on the air-dried gels which were determined to have varied amounts of mole ratios (3·0 to 4·5 mol of water to one mol of anhydrous oxide) and diffuse X-ray patterns classified as amorphous rings or halos with little or no structural information. The hydrothermal aging of such gels shows that these amorphous materials convert quite readily into crystalline hydrous lanthanide oxides which, when studied by X-ray diffraction methods, are characterized by a large number of sharp diffraction rings. Numerous studies have been done in order to elucidate the structural behavior of the lanthanides by means of X-ray crystal analysis. The crystal structures of the lanthanide oxides, oxyhydroxides, and trihydroxides have been reported and are fairly well understood as well as some other hydrous lanthanide oxide forms (Milligan, Mullica & Oliver, 1979; Milligan, Beall & Mullica, 1983).

Amorphous diffuse X-ray patterns contain structural information in the manner of an interatomic distance distribution. This distribution is computed from a measured X-ray diffraction pattern. The distribution is expressed as a radial distribution function (RDF) which furnishes information regarding the bond distances, the coordination number (CN), and the extent of ordering in the material under consideration. Noncrystalline compounds are deficient in long-range structural periodicity which is distinctive of crystalline solids. It is important that special care is taken during data collection and reduction procedures to minimize the introduction of spurious details into the distribution function for such uncertainties would undoubtedly mask true and real structural character.

Further, interest in amorphous materials has been increasing rapidly in the past several years. This interest, in part, stems from the technological potential in the areas of solid-state semi-conductors and catalysis. Part of the research program in this laboratory concerns the morphological and structural properties of the crystalline lanthanide trihydroxides and hydrous oxides. These studies have led to cooperative work dealing with several hydrous actinide oxides (Haire, Lloyd, Milligan & Beasley, 1977). Structural trends in the rare-earth trihydroxides (Beall, Milligan & Wolcott, 1977) have been observed and prompted studies of oxyhydroxides and other crystalline lanthanide compounds. These same observed trends have propagated investigations of the SRO structure of their precurser amorphous forms. The subject of this paper represents the first part of a major project

0108-7673/84/030264-06$01.50

dealing with all the amorphous hydrous lanthanide oxides and is expected to broaden the research base of SRO structural information by determining the coordination number, interatomic distances, and other pertinent factors associated with the SRO structure of amorphous hydrous erbium oxide.

Experimental

The starting material used in the preparation of the amorphous hydrous erbium oxide was obtained commercially as erbium sesquioxide (purity 99·9%). The oxide was dissolved in a stoichiometric amount of 6·0 mol dm^{-3} nitric acid. The resulting pink solution was subsequently filtered so as to remove any oxide still present and then cooled to 273 K. An excess of aqueous ammonia, also at 273 K, was then added to the solution using the rapid-mix method. In order to maintain an amorphous state, the precipitated gel was washed thoroughly with distilled ice water by refrigerated centrifugation until the amorphous material yielded a negative diphenylamine nitrate test. The gel was then spread on a glass plate so as to promote quick air drying. The elasped time from precipitation to drying was approximately 6 h. The dry material was finely ground until it passed through a 400-mesh sieve. The powder was desiccated while in a current of dry nitrogen gas for a period of 24 h. The sample was then transferred to a dry box under a positive nitrogen pressure. At that point, the amorphous erbium compound was pressed into a 2×4 cm sample holder until a mirror-like surface was observed under a light microscope.

Another portion of the dried erbium compound was used for physical and other experimental analyses. A Perkin–Elmer 521-grating IR spectrometer using the KBr pellet technique was employed to obtain an infrared spectrum over the range 4000–250 cm^{-1}. The spectrum displayed several characteristic absorption bands. One band in the hydroxyl region of 3400–3700 cm^{-1} is attributed to the O–H stretching frequency associated with hydrogen bonding. A second broad and pronounced band is observed around 1600 cm^{-1} which can be assigned to the deformation mode of water. Other important areas are the erbium–oxygen deformation band in the vicinity of 650 cm^{-1} and metal–hydroxyl stretching near 350 cm^{-1}. A thermal gravimetric analysis was also performed on the desiccated hydrous erbium oxide using a Perkin-Elmer TGS-1 thermobalance operating at 2·5 K min^{-1} while purging with nitrogen gas (20 cm^3 min^{-1}). The result of total dehydration was 4·08 (10) water molecules per formula unit of Er_2O_3. This corresponds to the basic formula $Er(OH)_3.0{\cdot}5H_2O$. The density (4·92 g cm^{-3}) of the powder sample was acquired through the use of a Quantachrome (model S.PY-1) stereopycnometer which utilizes the Archimedes principle of fluid displacement for volume determination. X-radiation fluorescence, applied to the same sample from which X-ray diffraction data was obtained, confirmed the presence of erbium and the absence of other possible metal contamination. This type of fluorescence analysis is dependent upon the solid-state detector which has been installed on the automated diffractometer and a multi-channel analyzer (MCA). The X-ray diffraction data was collected in a modified horizontal Siemens-K805 diffractometer. Modifications include the installation of a plastically bent sodium chloride crystal monochromator housed in a gold-plated chamber so as to prevent possible corrosion problems; a 3300 SP Kevex-ray Si(Li) energy-dispersive detector with an appropriate electronic counting chain to be discussed under *Data collection*; and a computerized system to control step-scan operations *via* the step-drive mechanism as well as data collection itself. The Kevex solid-state detector was checked for resolution (187 eV) and installed using a center of gravity installation over the sample housing for optimal balancing. The Si(Li) detector imposed no mechanical constraints.

Data collection

The sample holder containing the hydrous erbium oxide compound was mounted on the Siemens X-ray powder diffractometer. Scattered radiation from an Mo X-ray tube was incident on the housed NaCl monochromator aligned to scatter radiation with the wavelength of the Mo $K\alpha$ components onto the sample. Data was collected in the range $2 \leq 2\theta \leq 155°$ in a 2θ step-scan mode. A digital PDP 11/03 computer, by interfacing with an axis positioner, controls a stepping motor which steps up the detector in 0·1° 2θ increments. The signal from a Kevex 2000 preamplifier on the Kevex Si(Li) solid-state detector is processed by an Ortec 716-A amplifier and its output is directed to an Ortec 730 single-channel analyzer (SCA) which is set up to accept only the diffracted Mo $K\alpha$ radiation. At this point, the signal from the SCA is sent to both an Ortec 449 ratemeter which delivers it to a chart recorder for monitoring purposes and to a dual counter–timer which accumulates the counts and the elapsed time for the collection. 40 000 counts per step 2θ were collected, yielding a relative standard derivation of 0·5%. The position 2θ and time, which is internally converted to intensity, are deposited into computer storage. The counter–timer resets itself at each new position and collection continues according to the aforementioned counting-chain procedure. The control programs allow the options of varied step sizes or collected counts as well as a choice of scanning rates if a continuous scanning mode is desired.

The PDP 11/03 computer is programmed to make systematic checks on the primary beam intensity by

moving the detector, after a set interval of time or after ten steps 2θ, to a position selected as a standard intensity. A fast prescan of the diffraction profile identified the most intense band and thus the standard intensity was established. The use of a standard was deemed necessary owing to the length of the entire data-collection process, approximately two weeks. Any shifts in the standard intensity with time can be readily identified and the data then treated appropriately.

The output from the Ortec amplifier can also be directed, singularly or simultaneously, to an Ortec 6240B multichannel analyzer (MCA) with 4096 channels *via* an Ortec 433A dual sum and inverter. This arrangement was used for the X-ray fluorescence measurements mentioned earlier. This coupling of a solid-state detector to a multichannel analyzer not only permits qualitative and quantitative determinations of heavy constituents in a compound but also permits the option of energy-dispersive diffractometry when used with a broad-band beam (Wagner, Lee, Tai & Keller, 1980).Other uses of this type of instrumental arrangement are described elsewhere (Mullica, Beall, Milligan & Oliver, 1979).

Data analysis

Generally a structural analysis of an amorphous material is accomplished through the generation of an array of interatomic distances expressed as a radial distribution curve which is calculated from the experimental coherent scattering data. Many techniques, both experimental and mathematical, have been developed to improve the reliability of this type of analysis (Warren, 1969, 1975; Konnert & Karle, 1973).

The experimental data were first corrected for fluctuations in the intensity of the primary beam, as indicated by the standard. The intensity drift was found to be essentially linear and the maximum deviation was less than 0·1%, making this correction unnecessary. The polarization correction applied to raw data (I) was in the form given by Azaroff (1955):

$$P_{2\theta_2} = (1 + p\cos^2 2\theta_2)/(1 + p),$$

where $p = \cos^2 2\theta_1$ and θ_1 is the diffracting Bragg angle for the (200) plane of the NaCl monochromator crystal (for Mo $K\alpha$ $p = 0{\cdot}9375$) and θ_2 is the angle of diffraction for the sample. Next, a correction to minimize absorption effects was applied according to the method of Levy, Agron & Danford (1959). The experimental intensity 2θ values were interpolated to a function S defined as $4\pi \sin\theta/\lambda$, λ(Mo $K\bar{\alpha}$) = 0·71073 Å. The needed independent coherent scattering curve was then calculated as a function of S using the analytical atomic scattering factors, f_i, with appropriate anomalous dispersion correction terms for erbium and oxygen obtained from the usual source (*International Tables for X-ray Crystallography*, 1974). The scattering curve was modified following the procedure of Cromer & Liberman (1970). Normalization of the corrected experimental intensity data (I_c) to absolute electron units was accomplished by means of a high-angle method. The incoherent scattered intensity (I_{inc}), the Compton component, was calculated using the Compton scattering factors (Cromer, 1969) and the multiple-scattering contribution, double scatter only, was determined from the expressions given by Warren & Mozzi (1966). The total absorption coefficient of the sample components was high enough to make the multiple-scattering correction almost neglible. Both the Compton and multiple-scattering effects were subtracted from the normalized data. The final corrected experimental intensity curve, after being properly normalized, oscillates smoothly about the independent scattering curve, see Fig. 1.

From the normalized curve, one can calculate an interference function $Si(S)$, where $i(S)$ is defined as

$$i(S) = (I_c/N - I_b)/g^2(S),$$

where S is defined as $4\pi \sin\theta/\lambda$ and λ (Mo $K\bar{\alpha}$) = 0·71073 Å, N is a normalization factor, I_b is $\sum_{UC} f_i^2 + I_{inc}$, and $1/g^2(S)$ is a sharpening function chosen to be the sum of the squares of the scattering factors for a unit of composition. Fig. 2 displays the form of this interference function, $Si(S)$, after being exponentially dampened by a convergence variable factor in the form $\exp(-\alpha S^2)$, an introduced artificial temperature factor, where the value of α is 0·0005 Å^2. The application of the convergence factor, resulting in the exponential dampening of $Si(S)$ with respect to S, is necessary to reduce errors arising from the truncation of true upper limit of the transform to S_{max}.

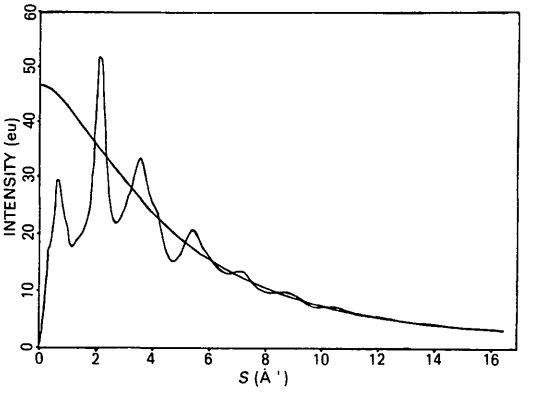

Fig. 1. The total X-ray diffraction pattern corrected for absorption, polarization, Compton and multiple scattering. Normalization was accomplished by a high-angle method about the independent scattering curve. Intensity measurements are in electron units (e.u.).

The Fourier sine transform of $Si(S)$ is in the form

$$rG(r) = 4\pi r^2[\rho(r) - \rho_a]$$
$$= 2r/\pi \int_0^{S_{max}} Si(S) \exp(-\alpha S^2) \sin(Sr)\, dS$$

and the RDF is expressed as

$$4\pi r^2\rho(r) = 4\pi r^2\rho_a + 2r/\pi \int_0^{S_{max}} Si(S) \times \exp(-\alpha S^2) \sin(Sr)\, dS,$$

where $\rho(r)$ is a density function and ρ_a is the average atomic density. Figs. 3 and 4 present plots of these distribution functions *versus* distance, r(Å).

Another form of distribution function which is used to reduce the termination errors relies on a resolution factor, Δ. This form of a RDF was designed by Lorch (1969). The suggested function is in the form

$$4\pi r^2[\rho(r) - \rho_a] = 2r/\pi \int_0^{S_{max}} i(S) \sin(Sr)/(\Delta/2) \times \sin(\Delta S/2)\, dS.$$

The resolution factor $\Delta = 2\pi/S_{max}$ was calculated to be 0·38 Å in this investigation. This technique yielded essentially the same results as seen in Figs. 3 and 4.

Discussion

The corrected experimental scattering curve, Fig. 1, oscillates smoothly about the independent scattering curve. This oscillation and the dampened motion about zero (see Fig. 2) of the interference function, $Si(S)$, lends credence to the fact that the scaling by the employed high-angle method was successful. The use of a monochromator, an intensity standard, and high counting time (40 000 counts per increment) ensured the collection of meaningful data and eliminated the need for any numerical filtering.

The reduced function, $rG(r)$, and the radial distribution function, $4\pi r^2\rho(r)$, are shown in Figs. 3 and 4, respectively. The utilization of the termination techniques previously described in data analysis appears effective, examine Fig. 4. At small radial distances, the RDF is featureless and, at large r values, it approaches the form of the average electron density curve. Some peak broadening is observed and can be attributed to the application of the convergence factor, but in the determination of coordination numbers it does not appear to be significant. The position of the first maximum in the RDF is found to be at 2·36 Å which represents the mean radius of the first coordination shell or the Er–O bond distance. The second peak is observed as a shoulder on the high r side of the first maxima. This peak was resolved by fitting the well defined first and third peaks to Gaussians and subtracting their sum from the experimental curve. The resulting peak, a well defined Gaussian,

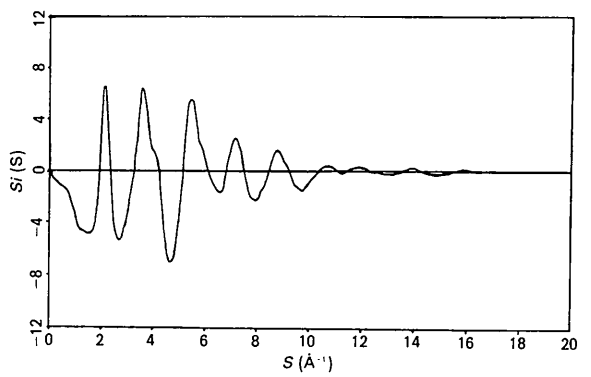

Fig. 2. The interference function $Si(S)$, in Å^{-1}, after exponential dampening by an artificial temperature factor of the form $\exp(-\alpha S^2)$ where $\alpha = 0{\cdot}0005$ Å^2.

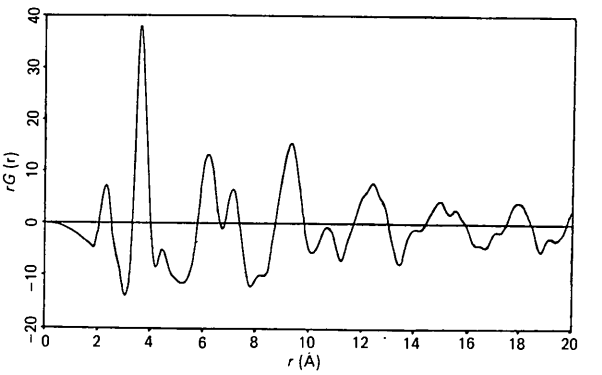

Fig. 3. The reduced distribution function $rG(r)$, in atoms Å^{-1}, resulting from the Fourier transform of $Si(S)$.

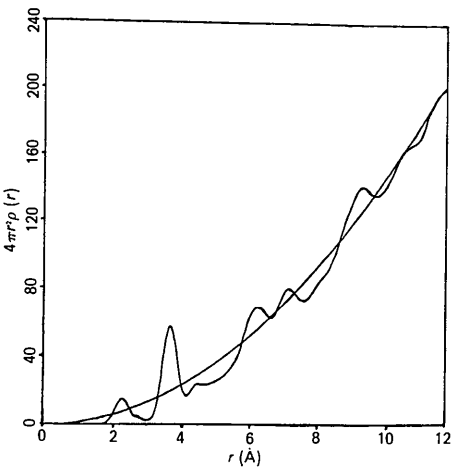

Fig. 4. The radial distribution function $4\pi r^2\rho(r)$, in atoms Å^{-1}, of hydrous erbium oxide and the average density curve $4\pi r^2\rho a$.

appears at 2·86 Å and is designated an oxygen–oxygen distance. The fitting of the Gaussians to the experimental RDF is shown in Fig. 5. The third peak occurs at 3·72 Å. This is the mean Er–Er interatomic distance. The coordination number about the metal can be calculated from the area under the first peak of the RDF. Calculation of this area from the fitted Gaussian yields a coordination number about the erbium of 9·05. Continuation of this process yields 8·23 oxygens at 2·86 Å from a central oxygen and 8·13 erbiums in the second coordination shell around an erbium at 3·72 Å.

The erbium-to-oxygen bond distance of 2·36 Å is quite reasonable when compared to other well defined systems. Table 1 presents bond distances and coordination numbers for several crystalline erbium compounds and experimental results obtained in this work. The O–O distance of 2·86 Å can be explained if one considers a D_{3h} tricapped trigonal prism geometry about an erbium center with all Er–O distances set at 2·36 Å. Calculation of the O–O distances between the apical oxygens with an O–Er–O angle of 75·8° results in a value of 2·90 Å. Fig. 6 shows a graphical representation of the density distribution in both crystalline $Er(OH)_3$ and ErOOH. These figures are the result of calculations based on Taylor's quasi-crystalline model (Taylor, 1979). This model calculation is a summation of atomic-unit (a.u.) contributions over all distances in the form

$$G'(r) = \sum_{i}^{\text{a.u.}} \sum_{j} N_{ij} 4\pi r^2 Q_{ij}(r).$$

$G'(r)$ is the total radial distribution function, where N_{ij} is related to the crystallographic multiplicity of site i divided by the number of formula units in the unit cell and the pair distribution function

$$4\pi r^2 Q_{ij}(r) = Z_i Z_j r / r_{ij} (1/2\pi b_{ij})^{1/2} \times \exp[-(r - r_{ij})^2 / 2b_{ij}],$$

Q is the number of formula units per Å^3 and Z is the number of electrons associated with each atom. The pair distribution function is a probability function used to locate considered atoms at a distance r. The values used for b_{ij} are calculated in part from isotropic thermal parameters. The thermal portion of b_{ij} is given by

$$b_{ij} = u_i^2 + u_j^2 = (B_i + B_j)/8\pi^2,$$

where u_i and u_j are the mean-square amplitudes of

Table 1. *Coordination numbers (CN) and bond distances* (Å)

Type	CN	Er–O$^{(1)}$	Er–O$^{(2)}$	Er–Er	Reference
Er_2O_3	6	2·31	—	3·98	(*a*)
$Er(OH)_3$	9	2·439 (3)	2·403 (3)	4·012	(*b*)
ErOOH	7	2·24 (6)	2·37 (5)	3·93	(*c*)
AHEO*	9	2·36	—	3·72	(*d*)

References: (*a*) Wyckoff (1960); (*b*) Beall *et al.* (1977); (*c*) Christensen (1965); (*d*) this work.
* Amorphous hydrous erbium oxide.

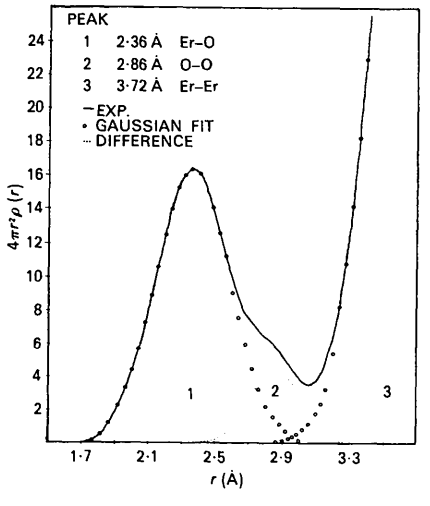

Fig. 5. Gaussian curves fitted to the RDF for resolution of an O–O peak. Arbitrary scaling was used on the abscissa for convenience of representation (units are atoms Å^{-1}).

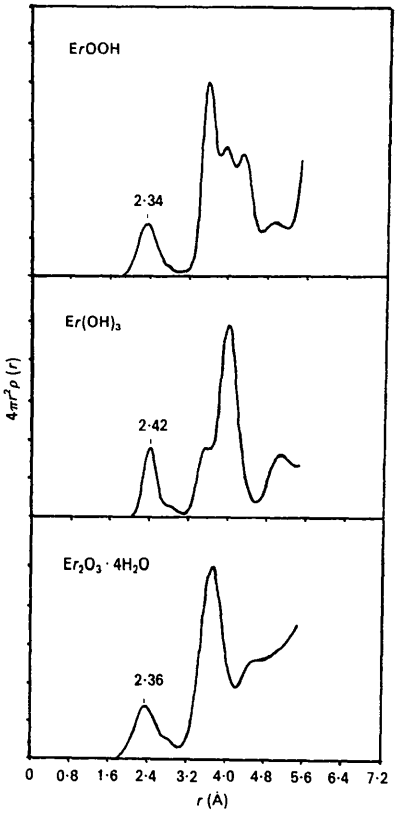

Fig. 6. Calculated distribution functions of crystalline ErOOH and $Er(OH)_3$ using Taylor's quasi-crystalline modeling equations and the experimental RDF. Arbitrary scaling was used on the abscissa for convenience of representation. Units are atoms Å^{-1},

vibration in Å of atoms i and j, and B_i and B_j are the isotropic thermal parameters. The values used in the calculation of ErOOH in Fig. 6 are those derived from the work of Christensen (1965). The density distribution of $Er(OH)_3$ was calculated from the thermal parameters as

$$U_{eq} = (U_{11}U_{22}U_{33})^{1/3} \quad \text{and} \quad B_{eq} = 8\pi^2 U_{eq}.$$

These thermal parameters were made available by Beall *et al.* (1977). A second term is added to b_{ij} to adjust for loss of pair correlation with increasing distance. This term is of the form

$$b_{ij},\ r = (r_{ij}/Kr_c)^2,$$

where K is a constant and r_c is 1 Å larger than the maximum r for the RDF calculation. The mean Er–O distance as shown in Fig. 6 is similar in the three systems amorphous hydrous erbium oxide, $Er(OH)_3$ and ErOOH. There is, however, a significant broadening of the first peak in the amorphous material when compared to that of the crystalline $Er(OH)_3$. This could imply a greater bond-length distribution in the amorphous sample or larger thermal parameters. Calculations of interference functions, RDF's and X-ray scattering curves for various nine-coordinated geometries are presently being performed on crystalline model systems in this laboratory. Further, it is believed by conjecture only that the studied erbium amorphous material could be a precursor to another form (termed in this lab as DR) which in turn transforms into $Er(OH)_3$ with ambient aging or with thermal aging. This DR form (Mullica, Milligan & Dillin, 1979) has not been structurally studied, but much effort is being spent to obtain meaningful structural data.

The authors thank the Robert A. Welch Foundation for financial support (grant No. AA-668). Further, the authors acknowledge appreciation for the help given by the facilities of Baylor University, Tarleton University and Arco Corp.

References

AZAROFF, L. V. (1955). *Acta Cryst.* **8**, 701–704.

BEALL, G. W., MILLIGAN, W. O. & WOLCOTT, H. A. (1977). *J. Inorg. Nucl. Chem.* **39**, 65–70.

CHRISTENSEN, A. N. (1965). *Acta Chem. Scand.* **19**, 1391–1396.

CROMER, D. T. (1969). *J. Chem. Phys.* **50**, 11, 4857–4859.

CROMER, D. T. & LIBERMAN, S. (1970). *J. Chem. Phys.* **53**, 5, 1891–1898.

DAMIENS, M. A. (1918). *Ann. Chem. (Warsaw)*, **10**, 137–183.

HAIRE, R. G., LLOYD, M. H., MILLIGAN, W. O. & BEASLEY, M. L. (1977). *J. Inorg. Nucl. Chem.* **39**, 843–847.

International Tables for X-ray Crystallography (1974). Vol. IV. Birmingham: Kynoch Press.

JOYE, P. & GARNIER, C. (1912). *C. R. Acad. Sci.* **154**, 510–522.

KONNERT, J. H. & KARLE, J. (1973). *Acta Cryst.* A**29**, 702–710.

LEVY, H. A., AGRON, P. A. & DANFORD, M. D. (1959). *J. Appl. Phys.* **30**, 2012–2013.

LORCH, E. (1969). *J. Phys. C*, **2**, 229–237.

MILLIGAN, W. O., BEALL, G. W. & MULLICA, D. F. (1983). *Crystallography in North America*, Sect. F, Ch. 9, pp. 362–369. American Crystallographic Association.

MILLIGAN, W. O., MULLICA, D. F. & OLIVER, J. D. (1979). *J. Appl. Cryst.* **12**, 411–412.

MULLICA, D. F., BEALL, G. W., MILLIGAN, W. O. & OLIVER, J. D. (1979). *J. Appl. Cryst.* **12**, 263–266.

MULLICA, D. F., MILLIGAN, W. O. & DILLIN, D. R. (1979). *J. Cryst. Growth*, **47**, 635–638.

TAYLOR, M. (1979). *J. Appl. Cryst.* **12**, 442–449.

WAGNER, C. N. J., LEE, D., TAI, S. & KELLER, L. (1980). *Advances in X-ray Analysis*, pp. 245–252. New York: Plenum Press.

WARREN, B. E. (1969). *X-ray Diffraction.* Reading, MA: Addison-Wesley.

WARREN, B. E. (1975). *J. Appl. Cryst.* **8**, 674–677.

WARREN, B. E. & MOZZI, R. L. (1966). *Acta Cryst.* **21**, 459–461.

WYCKOFF, R. W. R. (1960). *Crystal Structures*, Vol. 2. New York: Interscience.

Acta Cryst. (1984). A**40**, 269–277

Improvement of Protein Phases by Coarse Model Modification

BY V. YU. LUNIN AND A. G. URZHUMTSEV

Research Computer Centre, USSR Academy of Sciences, 142 292 Pushchino, Moscow Region, USSR

(*Received* 25 *April* 1983; *accepted* 2 *December* 1983)

Abstract

A procedure is suggested for the refinement of a set of protein phases and for its extension to a higher resolution, which is a development of the approach of Agarwal & Isaacs [*Proc. Natl Acad. Sci. USA*, (1977), **74**, 2835–2839]. A new set of phases is obtained by combining the starting phases with those calculated from a stereochemically non-conditioned coarse 'atomic' model which is automatically constructed and subjected to a least-squares refinement in reciprocal space. The method has been tested with actinidin data generated from atomic coordinates. Starting from the phases calculated to 3 Å resolution

0108-7673/84/030269-09$01.50